AD FALCON API Manual

MIT-S1 Model (Pestana & Whittle, 1999)

Javad Ghorbani

March 14, 2026

Contents

1 MIT-S1 Model (Pestana & Whittle, 1999) 3
1.1 Syntax . . . 3
1.2 Material parameters . . . 3
1.3 Custom state variables . . . 8
1.4 Stress invariants and notation . . . 9
1.5 LCC Compression Model (Eqs. 1–2) . . . 10
1.6 Critical-State Failure and Bounding Surface (Eqs. 3–5) . . . 10
1.7 Yield Gradient and Hardening (Eqs. 6–11) . . . 11
1.8 Non-Associated Flow and Consistency (Eqs. 12–14) . . . 12
1.9 Hysteretic Elasticity (Eqs. 15–21) . . . 12
1.10 Bounding-Surface Mapping for Overconsolidated States (Eqs. 22–25) . . . 13
1.11 Implementation Notes . . . 14
1.12 Single-Point Validation . . . 14
1.12.1 Prescribed K_0 consolidation effect on undrained clay response . . . 14
1.12.2 Anisotropy-rate effect in K_0-consolidated undrained clay . . . 14
1.13 References . . . 16

1 MIT-S1 Model (Pestana & Whittle, 1999)

MIT-S1 is a critical-state, bounding-surface constitutive model for soils. In FALCON it is available through the `MITS1Model` UMAT. This page summarizes the governing equations, input parameters, custom state variables, and the single-point benchmark cases included with the manual.

1.1 Syntax

This model is configured in `% Materials` as a user-defined mechanical material. Use `@UMAT:` with category `Mechanical` and pass the parameters as `name=value` pairs.

Example:

```
@UMAT: path/to/MITS1Model.cpp path/to/MITS1Model.hpp Mechanical \
    Pa=100 rho_c=0.25 p_ref=100 theta=0.20 \
    Cb=750 K0NC=0.50 nu0=0.25 omega=1.25 omega_s=4.0 \
    phi_cs=32 phi_mr=30 p=2.0 m=0.8 psi=30 \
    D=0 r=1 h=0 enableOCMapping=1 \
    P_min=1e-9 FTOL=1e-4 stressRelTol=1e-5 maxSubsteps=500 \
    CustomVariable=Alpha,b_xx,b_yy,b_zz,b_zy,b_zx,b_xy,alpha0_star,
alpha0_i,p_srp,srp_has_reversal,eta_srp_xx,eta_srp_yy,eta_srp_zz,
eta_srp_zy,eta_srp_zx,eta_srp_xy,eps_srp_xx,eps_srp_yy,eps_srp_zz,
eps_srp_zy,eps_srp_zx,eps_srp_xy
```

For readability, this example is wrapped across multiple lines; in input files you should write the full `@UMAT:` directive on a single line.

Example inputs used on this page:

- Generic `% Materials` snippet: `materials_mits1.txt`
- Pestana & Whittle (1999) Fig. 13-style K_0 undrained clay case: `pestana1999_fig13_ck0_strength_matching.txt`
- Pestana & Whittle (1999) Fig. 15-style K_0 undrained clay case: `pestana1999_fig15_ck0_psi30.txt`

1.2 Material parameters

Table 1. Core MIT-S1 material parameters

Symbol	Keyword in input	Required	Default	Role in the model
p_a	`Pa`	✓	none	Reference pressure used to normalise stiffness and stress levels in Eqs. (1), (15), and (19).
ρ_c	`rho_c`	✓	none	LCC compressibility; controls the slope of the limiting compression curve in Eq. (2) and enters isotropic hardening and flow through Eqs. (9), (13), and (25b).
p'_{ref}	`p_ref`	✓	none	Fixes the LCC position in Eq. (2), so it sets where isotropic compression and δ_b calculations are anchored.
θ	`theta`	✓	none	Transition exponent governing how quickly the response approaches the LCC in Eqs. (1), (8b), (9), and (25b).
C_b	`Cb`	✓	none	Elastic stiffness parameter controlling $K_{\max}$ and ρ_s in Eqs. (15) and (19).

Symbol	Keyword in input	Required	Default	Role in the model
K_0^{NC}	`K0NC`	✓	none	Defines the normally consolidated stress ratio and enters the anisotropy/flow scalars in Eqs. (8c) and (13).
ν_0	`nu0`	✓	none	Poisson ratio at stress reversal; sets the elastic ratio $2G_{\max}/K_{\max}$ in Eq. (15b) and the evolving ν in Eq. (18).
ω	`omega`	✓	none	Controls shear/Poisson degradation away from the SRP through Eqs. (16), (18), and (20).
ω_s	`omega_s`	✓	none	Controls small-strain shear degradation and the swelling slope in Eqs. (19b) and (20).
φ'_{cs}	`phi_cs`	✓	none	Critical-state friction angle; defines the failure surface in Eq. (3), the LCC coupling constant α_0^2 in Eq. (10), and the reference branch in Eq. (5).

Symbol	Keyword in input	Required	Default	Role in the model
φ'_{mr}	`phi_mr`	✓	none	Reference peak friction angle at $e = 1$; controls the aperture scalar through Eqs. (4c) and (5).
n_p	`p`	✓	none	Void-ratio exponent in Eq. (5); governs how strongly density changes the peak friction angle.
m	`m`	✓	none	Bounding-surface slenderness parameter; appears directly in the surface shape, flow, and mapping laws in Eqs. (4a), (7), (12a), and (24a).
ψ	`psi`	✓	none	Kinematic hardening rate of the anisotropy tensor $\boldsymbol{b}$ in Eq. (7); it controls how fast the surface translates.
D	`D`	×	`0`	Hysteretic swelling contribution after stress reversal in Eq. (19b).
r	`r`	×	`1`	Exponent controlling the decay of the hysteretic term $D(1-\mu^r)$ in Eq. (19b).

Symbol	Keyword in input	Required	Default	Role in the model
h	h	×	0	Overconsolidated mapping modulus scale in Eq. (25b).

Table 2. Numerical and advanced controls

Keyword in input	Required	Default	Role
P_min	✓	none	Positive floor for p' and α' to avoid singular stress-ratio updates.
FTOL	✓	none	Admissibility tolerance for the yield function and local correction steps.
stressRelTol	×	1e-5	Relative stress target used by the adaptive substepping error estimator.
maxSubsteps	×	500	Maximum number of internal substeps per increment.
enableOCMapping	×	1	Enables the interior bounding-surface mapping of Eqs. (22)–(25).
Alpha_max	×	1e12	Safety cap on α' during numerical integration.
hardeningRateCap	×	50	Caps logarithmic hardening rates as a numerical safeguard.
alphaOverPMax	×	0	Optional cap on α'/p'; 0 disables the cap.
alphaCapScale	×	0	Optional LCC-based cap on α' growth; 0 disables it.
initOverride	×	0	Rebuilds internal state from the current stress/void-ratio state during conditioning.
initOCR	×	1	OCR-style scale used when initOverride=1.

Keyword in input	Required	Default	Role
`initBScale`	×	`1`	Scale factor for rebuilding b from the current stress ratio.
`initAlphaMode`	×	`1`	Chooses how conditioning reconstructs α' from the current state.
`initEnforceAdmissible`	×	`1`	Enlarges α' during conditioning if the current state is inadmissible.

1.3 Custom state variables

Declare custom state variables using `CustomVariable=` so they are stored for restart/output.

Table 3. MIT-S1 custom variables

Keyword(s)	State variable	Required	Role
`Alpha`	α'	✓	Current bounding-surface size used in Eqs. (4a), (6b), (6c), (8b), and (12), and updated by Eqs. (9) to (11).
`b_xx`, `b_yy`, `b_zz`, `b_zy`, `b_zx`, `b_xy`	b	✓	Components of the anisotropy tensor that translate the surface in Eq. (4a) and evolve through Eq. (7).
`alpha0_star`	α_0^*	✓	Current constant-η image-point size from Eq. (24a), used in the mapping factor g_1 in Eq. (24).

Keyword(s)	State variable	Required	Role
`alpha0_i`	α_{0i}	✓	First-yield loading-surface size used with α_0^* in Eq. (24) during overconsolidated mapping.
`p_srp`	p'_{srp}	✓	Mean effective stress at the stored stress-reversal point, used in Eqs. (16), (17), and (19b).
`srp_has_reversal`	SRP flag	✓	Indicates whether the stress-reversal-point history has been initialized for the hysteretic elasticity update.
`eta_srp_xx`, `eta_srp_yy`, `eta_srp_zz`, `eta_srp_zy`, `eta_srp_zx`, `eta_srp_xy`	$\boldsymbol{\eta}_{\mathrm{srp}}$	✓	Stress-ratio tensor at the stress-reversal point, used to evaluate m_4 in Eq. (17).
`eps_srp_xx`, `eps_srp_yy`, `eps_srp_zz`, `eps_srp_zy`, `eps_srp_zx`, `eps_srp_xy`	$\boldsymbol{\varepsilon}_{\mathrm{srp}}$	✓	Strain tensor at the stress-reversal point, used by the loading-unloading detector in Eq. (21).

1.4 Stress invariants and notation

Stress invariants are written in effective-stress form:

$$p' = \tfrac{1}{3}\,\mathrm{tr}(\boldsymbol{\sigma}'), \qquad \boldsymbol{s} = \boldsymbol{\sigma}' - p'\boldsymbol{I}, \qquad \boldsymbol{\eta} = \frac{\boldsymbol{s}}{p'}. \tag{o}$$

The third invariant of the stress-ratio tensor is

$$J_3^{\eta} = \det(\boldsymbol{\eta}) = \frac{\det(\boldsymbol{s})}{(p')^3}. \tag{oa}$$

The internal variables are the void ratio e, the scalar bounding-surface size α', and the deviatoric anisotropy tensor $\boldsymbol{b}$.

Plastic flow is written as

$$d\boldsymbol{\varepsilon}^p = d\lambda\,\boldsymbol{P}, \qquad d\varepsilon_v^p = d\lambda\,P_p, \qquad d\boldsymbol{\varepsilon}_d^p = d\lambda\,\boldsymbol{P}_s. \tag{0b}$$

1.5 LCC Compression Model (Eqs. 1–2)

For hydrostatic first loading:

$$d\varepsilon_v = \frac{e}{1+e}\left[\frac{\delta^\theta}{C_b\left(\dfrac{p'}{p_a}\right)^{1/3}} + \frac{\rho_c}{\left(\dfrac{p'}{p_a}\right)}\left(1-\delta^\theta\right)\right]\frac{dp'}{p_a}, \tag{1a}$$

$$d\varepsilon_v^e = \frac{e}{1+e}\,\frac{1}{C_b\left(\dfrac{p'}{p_a}\right)^{1/3}}\,\frac{dp'}{p_a}. \tag{1b}$$

The LCC distance measure is

$$\delta = 1 - \frac{p'}{p'_b}, \qquad p'_b = p'_{\mathrm{ref}}\left(\frac{1}{e}\right)^{1/\rho_c}. \tag{2}$$

1.6 Critical-State Failure and Bounding Surface (Eqs. 3–5)

The Matsuoka-Nakai critical-state failure function is

$$h_f(\boldsymbol{\eta}) = k^2 - \boldsymbol{\eta} : \boldsymbol{\eta} = 0, \tag{3a}$$

with

$$k^2 = k_a^2 + \left(3 - \frac{k_a^2}{2}\right)J_3^\eta, \qquad k_a^2 = \frac{8\sin^2\varphi'_{cs}}{3+\sin^2\varphi'_{cs}}. \tag{3b}$$

The distorted lemniscate bounding surface is

$$f = (p')^2\left[(\boldsymbol{\eta}-\boldsymbol{b}) : (\boldsymbol{\eta}-\boldsymbol{b}) - \zeta^2\left(1 - \left(\frac{p'}{\alpha'}\right)^m\right)\right] = 0, \tag{4a}$$

$$\zeta^2 = c^2 + \boldsymbol{b} : \boldsymbol{b} - 2\,\boldsymbol{\eta} : \boldsymbol{b}, \tag{4b}$$

$$c^2 = c_a^2 + \left(3 - \frac{c_a^2}{2}\right)J_3^\eta, \qquad c_a^2 = \frac{8\sin^2\varphi'_m}{3+\sin^2\varphi'_m}. \tag{4c}$$

The density-dependent peak friction angle is

$$\frac{1}{\tan\varphi'_m} = \frac{1}{\tan\left(45^\circ + \dfrac{\varphi'_{cs}}{2}\right)} + \left[\frac{1}{\tan\varphi'_{mr}} - \frac{1}{\tan\left(45^\circ + \dfrac{\varphi'_{cs}}{2}\right)}\right] e^{n_p}. \tag{5}$$

Here e^{n_p} means void ratio raised to the power n_p, not an exponential.

1.7 Yield Gradient and Hardening (Eqs. 6–11)

Define

$$\boldsymbol{Q} = \frac{\partial f}{\partial \boldsymbol{\sigma}'} \equiv (Q_p, \boldsymbol{Q}_s). \tag{6a}$$

With $g = (p'/\alpha')^m$, the components used in the UMAT are

$$Q_p = p'\left[(m\zeta^2 + 2\,\boldsymbol{\eta} : \boldsymbol{b})g - 2\,\boldsymbol{\eta} : \boldsymbol{\eta} + \left(9 - \frac{3c_a^2}{2}\right)(1-g)J_3^{\eta}\right], \tag{6b}$$

$$\boldsymbol{Q}_s = p'\left[2(\boldsymbol{\eta} - g\boldsymbol{b}) - \left(3 - \frac{c_a^2}{2}\right)(1-g)\frac{\partial J_3^{\eta}}{\partial \boldsymbol{\eta}}\right]. \tag{6c}$$

Kinematic hardening of the anisotropy tensor follows

$$d\boldsymbol{b} = \psi\,\frac{1+e}{e\,\alpha'}\left[\frac{r_x}{m}\left\langle Q_p\, d\varepsilon_v^p\right\rangle + r_y\left|\boldsymbol{Q}_s : d\varepsilon_d^p\right|\right](\boldsymbol{\eta} - \boldsymbol{b}), \tag{7}$$

with Macaulay brackets $\langle x\rangle = \max(x, 0)$ and

$$r_x = \frac{k^2 + \boldsymbol{b} : \boldsymbol{b} - 2\,\boldsymbol{\eta} : \boldsymbol{b}}{k_a^2}, \tag{8a}$$

$$r_y = \left(d^2 + \boldsymbol{b} : \boldsymbol{b} - 2\,\boldsymbol{\eta} : \boldsymbol{b}\right)\left[1 + \left(\frac{\alpha'}{p'} - 1\right)\delta_b^{\theta}\right], \tag{8b}$$

$$d^2 = d_a^2 + \left(3 - \frac{d_a^2}{2}\right)J_3^{\eta}, \qquad d_a^2 = \frac{2(1 - K_0^{NC})^2}{1 + K_0^{NC} + (K_0^{NC})^2}. \tag{8c}$$

The isotropic hardening law for α' is

$$\frac{d\alpha'}{\alpha'} = \frac{1+e}{e(\rho_c - \rho_s)(1-\delta_b)^{\theta}}\left[d\varepsilon_v^p + \delta_b^{\theta}\left(\frac{\boldsymbol{Q}_s : d\boldsymbol{\varepsilon}_d^p}{p'}\right)\right] - \frac{2\,\boldsymbol{b} : d\boldsymbol{b}}{\alpha_0^2 + \boldsymbol{b} : \boldsymbol{b}}, \tag{9}$$

where

$$\delta_b = 1 - \frac{\alpha'}{p'_b}\left(1 + \frac{\boldsymbol{b} : \boldsymbol{b}}{\alpha_0^2}\right), \qquad \alpha_0^2 = 24\left(\frac{\sin\varphi'_{cs}}{3 - \sin\varphi'_{cs}}\right)^2. \tag{10}$$

In the LCC regime ($\delta_b = 0$),

$$\frac{d\alpha'}{\alpha'} = \frac{1+e}{e(\rho_c - \rho_s)}\, d\varepsilon_v^p - \frac{2\,\boldsymbol{b} : d\boldsymbol{b}}{\alpha_0^2 + \boldsymbol{b} : \boldsymbol{b}}. \tag{11}$$

1.8 Non-Associated Flow and Consistency (Eqs. 12–14)

The volumetric flow component is

$$P_p = \begin{cases} (k^2 - \boldsymbol{\eta} : \boldsymbol{\eta})\dfrac{p'}{\alpha'}(1-\delta_b)^m, & \boldsymbol{\eta} : \boldsymbol{\eta} \le k^2, \\ (k^2 - \boldsymbol{\eta} : \boldsymbol{\eta})\dfrac{p'}{\alpha'}, & \boldsymbol{\eta} : \boldsymbol{\eta} > k^2, \end{cases} \tag{12a}$$

and the deviatoric flow component is

$$\boldsymbol{P}_s = x\, P_p\, \boldsymbol{\eta} + \frac{\zeta^2 \|\boldsymbol{\eta}\|}{\alpha'}\, \boldsymbol{Q}_s. \tag{12b}$$

The coefficient imposing the K_0^{NC} constraint is

$$x = \left(\frac{\rho_c}{\rho_c - \rho_s}\right)\left[\frac{1 + 2K_0^{NC}}{3(1 - K_0^{NC})} - \frac{K}{2G}\frac{\rho_s}{\rho_c}\right]. \tag{13}$$

Consistency gives

$$d\lambda\, H = -\frac{\partial f}{\partial \alpha'}\, d\alpha' - \frac{\partial f}{\partial \boldsymbol{b}} : d\boldsymbol{b}, \tag{14a}$$

$$d\lambda = \frac{K Q_p\, d\varepsilon_v + 2G\, \boldsymbol{Q}_s : d\boldsymbol{\varepsilon}_d + \dfrac{\partial f}{\partial e}(1+e)\, d\varepsilon_v}{H + K Q_p P_p + 2G\, \boldsymbol{Q}_s : \boldsymbol{P}_s}. \tag{14b}$$

1.9 Hysteretic Elasticity (Eqs. 15–21)

At the stress-reversal point,

$$\frac{K_{\max}}{p_a} = C_b \left(\frac{1+e}{e}\right)\left(\frac{p'}{p_a}\right)^{1/3}\left(1 + \frac{K_{\max}}{2G_{\max}}\, \boldsymbol{\eta} : \boldsymbol{\eta}\right)^{1/6}, \tag{15a}$$

$$\frac{2G_{\max}}{K_{\max}} = 3\left(\frac{1 - 2\nu_0}{1 + \nu_0}\right). \tag{15b}$$

The shear/bulk ratio degrades with distance from the SRP:

$$\frac{(2G/K)}{(2G_{\max}/K_{\max})} = \begin{cases} \dfrac{1}{1+\omega m_4}, & p' < p'_{\mathrm{srp}}, \\ \dfrac{1}{1+\omega\mu m_4}, & p' \geq p'_{\mathrm{srp}}, \end{cases} \tag{16}$$

with

$$\mu = \begin{cases} p'/p'_{\mathrm{srp}}, & p' < p'_{\mathrm{srp}}, \\ p'_{\mathrm{srp}}/p', & p' \geq p'_{\mathrm{srp}}, \end{cases} \qquad m_4 = \left[(\boldsymbol{\eta} - \boldsymbol{\eta}_{\mathrm{srp}}) : (\boldsymbol{\eta} - \boldsymbol{\eta}_{\mathrm{srp}})\right]^{1/2}. \tag{17}$$

The equivalent Poisson ratio is

$$\nu = \nu_0 + \frac{\frac{1}{3}\omega m_4(1+\nu_0)}{1+\frac{2}{3}\omega m_4(1+\nu_0)}, \qquad \nu_0 \leq \nu < 0.5. \tag{18}$$

The tangent bulk modulus and swelling slope are

$$\frac{K}{p_a} = \frac{1+e}{e\,\rho_s}\frac{p'}{p_a}, \tag{19a}$$

$$\rho_s = D(1-\mu^r) + \frac{1+\omega_s m_4}{C_b}\left(1 + \frac{K_{\max}}{2G_{\max}}\,\boldsymbol{\eta} : \boldsymbol{\eta}\right)^{1/6}\left(\frac{p'}{p_a}\right)^{2/3}. \tag{19b}$$

and the small-strain shear reduction is

$$\frac{G}{G_{\max}} = \frac{1}{(1+\omega m_4)(1+\omega_s m_4)}. \tag{20}$$

The SRP is identified from the strain increment relative to the previous reversal state:

$$s\,ds = \begin{cases} \Delta\varepsilon_v\, d\varepsilon_v, & d\varepsilon_v \neq 0, \\ \Delta\boldsymbol{\varepsilon}_d : d\boldsymbol{\varepsilon}_d, & d\varepsilon_v = 0, \end{cases} \qquad \begin{cases} ds > 0 & \text{loading}, \\ ds < 0 & \text{unloading (new SRP)}. \end{cases} \tag{21}$$

1.10 Bounding-Surface Mapping for Overconsolidated States (Eqs. 22–25)

Loading is detected from the image-point gradient:

$$K Q_p^I\, d\varepsilon_v + 2G\,\boldsymbol{Q}_s^I : d\boldsymbol{\varepsilon}_d \begin{cases} \geq 0 & \text{loading}, \\ < 0 & \text{unloading}. \end{cases} \tag{22}$$

When mapping is active,

$$\boldsymbol{P} = (1-g_1)\boldsymbol{P}^I + g_1\boldsymbol{P}_0, \tag{23a}$$

$$H = \langle H^I \rangle + H_0\frac{g_1}{1-g_1}\left(1 - \frac{\boldsymbol{\eta} : \boldsymbol{\eta}}{c^2}\right)^{1/2}, \tag{23b}$$

$$g_1 = \frac{\alpha' - \alpha_0^*}{\alpha' - \alpha_{0i}}, \qquad 0 \le g_1 \le 1, \tag{24}$$

with first-yield quantities

$$P_{0p} = -2\|\boldsymbol{\eta} - \boldsymbol{b}\| \left\| \frac{\boldsymbol{s}^I}{\alpha'} \right\|, \qquad \boldsymbol{P}_{0s} = \boldsymbol{P}_s^I, \tag{25a}$$

$$H_0 = \left(\frac{\rho_s^I}{\rho_c - \rho_s^I} \right) \frac{h}{1 - \delta_b^\theta} K_{\max}^I \|\boldsymbol{Q}^I\| \|\boldsymbol{P}^I\|. \tag{25b}$$

The loading-surface size stored in `alpha0_star` is evaluated from the constant-$\boldsymbol{\eta}$ image-point relation

$$\alpha_0^* = \frac{p'}{(g^*)^{1/m}}, \qquad g^* = 1 - \frac{(\boldsymbol{\eta} - \boldsymbol{b}) : (\boldsymbol{\eta} - \boldsymbol{b})}{\zeta^2}. \tag{24a}$$

1.11 Implementation Notes

- The constitutive equations above define the model. In the public FALCON interface, MIT-S1 uses explicit adaptive substepping for local stress integration.

1.12 Single-Point Validation

This page includes two K_0-undrained single-point benchmark reproductions based on Pestana & Whittle (1999). The figures compare the data reported in that paper with the corresponding FALCON MIT-S1 responses.

1.12.1 Prescribed K_0 consolidation effect on undrained clay response

The first reproduction follows the clay benchmark reported in Pestana & Whittle (1999) Figure 13. The figure compares the paper data with the FALCON MIT-S1 response for the same parameter sets.

Use `pestana1999_fig13_ck0_strength_matching.txt` as the starting deck and vary `phi_mr`, `m`, and the sign of `dEpsAxial` to recover the different compression/extension branches.

1.12.2 Anisotropy-rate effect in K_0-consolidated undrained clay

The second reproduction follows Pestana & Whittle (1999) Figure 15, which isolates the effect of the anisotropy-rate parameter ψ for K_0-consolidated clay. The figure compares the paper data with the FALCON MIT-S1 response.

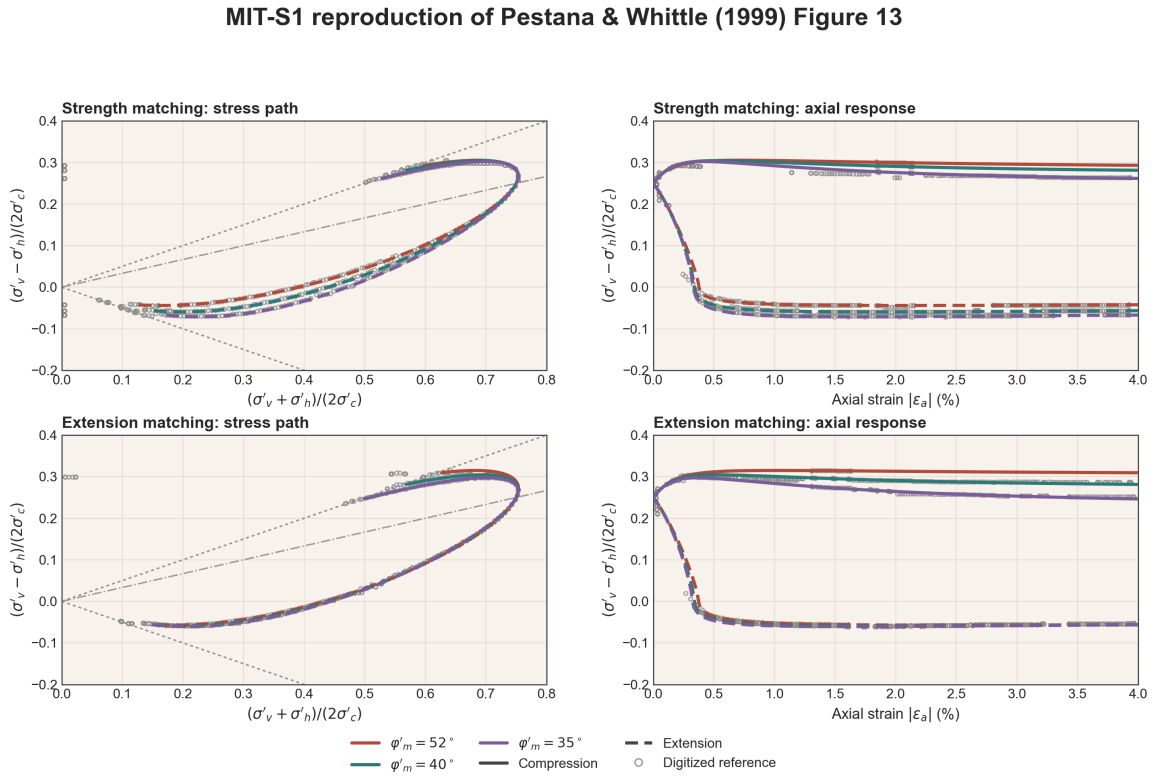

Figure 1: MIT-S1 alternate reproduction of Pestana and Whittle 1999 Figure 13

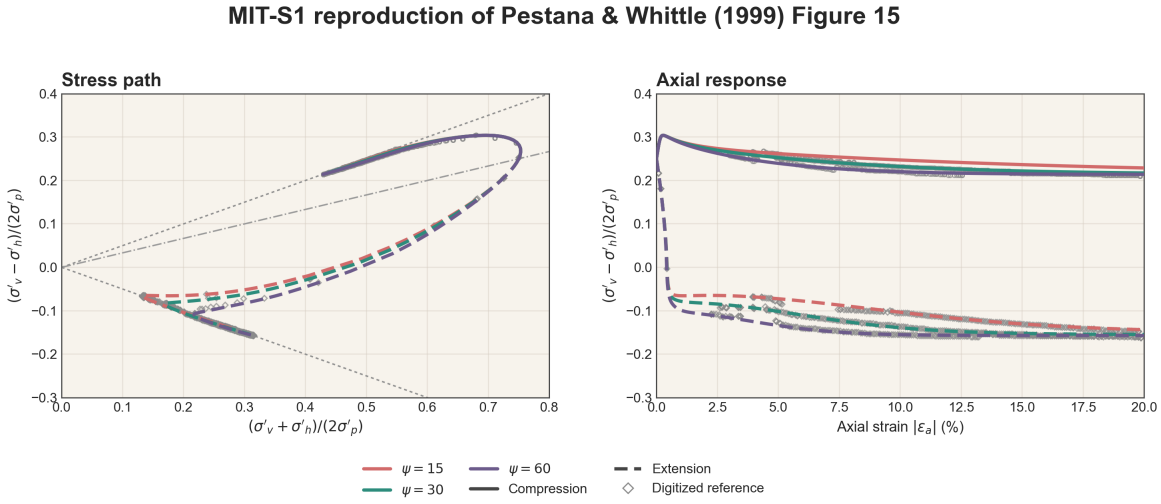

Figure 2: MIT-S1 alternate reproduction of Pestana and Whittle 1999 Figure 15

The sample deck `pestana1999_fig15_ck0_psi30.txt` reproduces the middle $\psi = 30$ case; sweep `psi = 15, 30, 60` to rebuild the full family.

1.13 References

- Pestana, J. M., & Whittle, A. J. (1999). *Formulation of a unified constitutive model for clays and sands. International Journal for Numerical and Analytical Methods in Geomechanics*, 23, 1215–1243.